Low-complexity, Sub-band DPD with Sequential Learning

Novel Algorithms and WarpLab Implementation

Chance Tarver · Mahmoud Abdelaziz · Lauri Anttila · Mikko Valkama · Joseph R. Cavallaro

Abstract Digital predistortion (DPD) is an effective way of mitigating spurious emission violations without the need of a significant power reduction in the transmitter, thus providing better power efficiency and network coverage. In this paper an iterative version of the IM3 sub-band DPD, proposed earlier by the authors, is presented. The DPD learning is iterated between the higher and lower IM3 sub-bands until a satisfactory performance is achieved for both of them. A sequential DPD learning procedure is also presented in order to reduce the hardware complexity when higher order nonlinearities are incorporated in the DPD learning. Improvements on the convergence speed of the adaptive DPD learning are also achieved via incorporating a variable learning rate and training from previous values. A WarpLab implementation of the proposed DPD is also shown with excellent suppression of the targeted spurious emissions.

Keywords Adaptive filters · carrier aggregation · digital predistortion · nonlinear distortion · power amplifier · software-defined radio · spectrally-agile radio · spurious emission.

1 Introduction

In mobile devices transmitting spectrally aggregated carriers with a single power amplifier (PA), some of the intermodulation distortion (IMD) components created

Chance Tarver and Joseph R. Cavallaro
Department of Electrical and Computer Engineering
Rice University, Houston, TX, 77005, USA
E-mail: {cat12,cavallar}@rice.edu

Mahmoud Abdelaziz, Lauri Anttila and Mikko Valkama
Department of Electronics and Communication Engineering
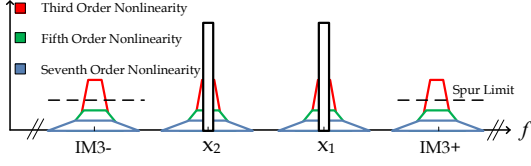Tampere University of Technology, Finland

by the nonlinear PA will fall on the spurious region as shown in Fig. 1 and may seriously violate the spurious emission limits [?,?,?,?]. To satisfy the stringent emission requirements in such scenarios, devices may need to considerably back off their transmit power from the nominal maximum value (e.g., +23 dBm in 3GPP LTE uplink). However, reducing the transmit power in order to fulfill the emission mask will necessarily reduce the uplink coverage. An alternative solution to power back-off is to use digital predistortion (DPD) for reducing the unwanted spectral emissions [?,?,?,?,?].

In [?], the third-order IMD at the IM3± sub-bands were considered separately, while not taking into consideration the mutual effect of each of the IM3 sub-band DPDs over the other. An FPGA implementation of this solution has also been presented by the authors in [?] demonstrating real-time processing of the adaptive DPD learning solution. An extension of the DPD solution in [?,?] is proposed in this paper, where an iterative learning algorithm is used between the two IM3 sub-bands until they are both properly suppressed. Moreover, in [?], higher nonlinearity orders were introduced in addition to the third-order nonlinearity processing in [?,?]. A WarpLab implementation of an iterative version of this higher order sub-band DPD is also presented in this paper with additional ideas added to reduce the complexity and/or improve the learning speed of the proposed DPD. In summary, the main novelty of this paper is as follows:

- Introducing an iterative version of the previously proposed sub-band DPD. This solution iterates between the different spurious components, such as the IM3+ and IM3-, until a satisfactory performance is achieved for each of them.
- The learning of the higher order nonlinearities in each sub-band is done sequentially, one basis func-

Fig. 1 Power spectral density of a carrier aggregated signal after being applied through a nonlinear PA. Nonlinearity orders up to the seventh are shown, and only IM3± spurious emissions are presented as they are the main focus of this work.

tion at a time in ascending order. This has the advantage of reducing the hardware complexity by essentially using one learning module for all the nonlinearity orders. An additional flexibility advantage is that we can stop adding higher orders in the learning phase once a sufficient spurious emission suppression is achieved, thus further reducing the complexity.

– In order to improve the convergence speed of the proposed solution, two modifications have been introduced in this paper. The first is using a variable learning rate during the DPD coefficient learning to have a fast convergence at the initial phase of the learning while not sacrificing the steady state error. The second modification is that the DPD coefficients are stored once they are converged, and act as a starting point for learning once the same carrier configuration is transmitted again.

– A WarpLab implementation of the proposed solution is done demonstrating effective performance of the proposed solution using real hardware equipment.

This paper is organized as follows. In Section II, the modeling of the spurious emissions at the IM3 sub-bands and their mutual effects are presented. The proposed iterative sub-band DPD processing is also introduced in this section. In Section III, sequential learning of the DPD coefficients is proposed to reduce the hardware complexity. In Section IV, two methods are proposed for improving the convergence time. In Section V, the overall DPD system flow is presented. In Section VI, we show the results from testing the proposed algorithms on the WarpLab platform. Finally, in Section VII, we conclude the paper.

2 Spurious Component Modeling and Iterative IM3 Sub-band DPD Processing

In [**?**], a decorrelation-based sub-band DPD was proposed to mitigate the spurious emissions at the IM3± sub-bands. However, the mutual effect of, for example, the IM3+ sub-band DPD on the IM3- sub-band was

not taken into consideration. In this work, we propose an iterative sub-band DPD that starts with linearizing the IM3+ sub-band, and then after applying the IM3+ sub-band DPD, the learning is switched to the IM3- sub-band. Since each of the IM3± sub-band DPDs has an effect on the other sub-band, the proposed DPD iterates the learning between the two sub-bands until both spurious emissions are sufficiently suppressed.

To further illustrate this behavior, a mathematical analysis is introduced in this section to show the impact of the IM3+ sub-band DPD on the IM3- sub-band when a dual carrier signal is applied to a nonlinear PA. This analysis will provide a theoretical foundation and motivation for our work. For simplicity of the presentation, we restrict our analysis in this section to third-order nonlinearity. However, in the actual WarpLab experiments, higher order nonlinearities are included in the DPD processing. The analysis is carried out at composite baseband equivalent level, and the two component carriers (CC's) are assumed to be separated by $2f_{IF}$. Thus, the composite baseband equivalent PA input and output signals, $x(n)$ and $y(n)$, read

$$x(n) = x_1(n)e^{j2\pi \frac{f_{IF}}{f_s}n} + x_2(n)e^{-j2\pi \frac{f_{IF}}{f_s}n}, \quad (1)$$

$$y(n) = \beta_1 x(n) + \beta_3 |x(n)|^2 x(n), \quad (2)$$

where β_1 and β_3 are unknown PA coefficients, and $x_1(n)$ and $x_2(n)$ are the baseband equivalents of the input CCs. Through direct substitution of (1) in (2), the baseband equivalent positive and negative IM3 terms read

$$y_{IM3_+}(n) = \beta_3 x_2^*(n) x_1^2(n), \quad (3)$$

$$y_{IM3_-}(n) = \beta_3 x_1^*(n) x_2^2(n). \quad (4)$$

The idea proposed in [**?**], for suppressing the IMD at the IM3+ sub-band for example, is to inject a proper additional low-power cancellation signal to (1), located at three times f_{IF}, such that spurious emission at the IM3+ sub-band at the PA output is suppressed. Stemming from the signal structure in (3), the injection signal is of the form $x_2^*(n) x_1^2(n)$ but should be scaled properly with a complex DPD coefficient denoted here by α. Thus, incorporating such DPD processing, the composite baseband equivalent PA input signal now reads

$$\tilde{x}(n) = x_1(n)e^{j2\pi \frac{f_{IF}}{f_s}n} + x_2(n)e^{-j2\pi \frac{f_{IF}}{f_s}n}$$
$$+ \alpha(x_2^*(n) x_1^2(n))e^{j2\pi \frac{3f_{IF}}{f_s}n}. \quad (5)$$

Substituting now $\tilde{x}(n)$ in (2), the IM3 components at PA output read

$$
\begin{aligned}
\tilde{y}_{IM3_+}(n) = {} & (\beta_3 + \beta_1\alpha)x_2^*(n)x_1^2(n) \\
& + 2\beta_3\alpha(|x_1(n)|^2 + |x_2(n)|^2)x_2^*(n)x_1^2(n) \\
& + \beta_3|\alpha|^2\alpha|x_1(n)|^4|x_2(n)|^2x_2^*(n)x_1^2(n), \quad (6)
\end{aligned}
$$

$$
\tilde{y}_{IM3_-}(n) = \beta_3 x_1^*(n)x_2^2(n) + \boxed{2\beta_3\alpha^*|x_1(n)|^2x_1^*(n)x_2^2(n)}. \tag{7}
$$

It can be seen from (6) and (7) that the spurious emissions at both IM3 sub-bands are dependent on the DPD parameter α, despite the cancellation signal being injected only at the IM3+ sub-band. In particular, an additional fifth-order term which depends on α appears at the IM3- sub-band, which is shown inside the box in (7). Despite the magnitude of this term being quite small, it becomes considerable when the PA exhibits strong nonlinearities. This represents the theoretical basis of the mutual effect the IM3+ sub-band DPD has on the two IM3 sub-bands.

In [?], the learning of the DPD parameter α, for the IM3+ sub-band, for example, was formulated to minimize the correlation between the IMD at the considered IM3 sub-band and the distortion basis $x_2^*(n)x_1^2(n)$. This correlation minimization will eventually minimize the distortion at the considered sub-band effectively, as demonstrated in [?,?]. However, optimizing the DPD parameter α to minimize the power at the IM3+ sub-band, will affect the IM3- sub-band as well, as shown in (6) and (7). That is why an iterative sub-band DPD learning is proposed in this paper, in the case both IM3 sub-bands are required to be mitigated effectively. First we start by learning the DPD coefficients for the IM3+ sub-band, then after injecting the IM3+ cancellation signal, the emissions at the IM3- sub-band are raised a little above their original levels due to the mutual effect described earlier. Then, the DPD learning is switched to the IM3- sub-band, which then also affects the IM3+ sub-band. That is why an extra iteration is required at the IM3+ sub-band such that the spurious emissions are reduced at both IM3 sub-bands. This will be demonstrated in the WARPLab experimental results in Section 6.

In the following sections, modifications are introduced to the proposed sub-band DPD in order to reduce the complexity, improve the convergence speed, or both. These aspects are particularly important for mobile devices, which is the main scope of this work.

3 Sequential Learning of IM3 sub-band DPD Coefficients

A detailed analysis of the nonlinear distortions at the IM3 sub-band has been done in [?] when a ninth-order PA is excited with a dual carrier signal as in (1). We hereby present the distortion components up to the ninth order at the IM3+ sub-band, which read

$$
u_3^+(n) = x_2^*(n)x_1^2(n), \tag{8}
$$
$$
u_5^+(n) = u_3^+(n) \times (2|x_1(n)|^2 + 3|x_2(n)|^2), \tag{9}
$$
$$
\begin{aligned}
u_7^+(n) = u_3^+(n) \times {} & (3|x_1(n)|^4 + 6|x_2(n)|^4 \\
& + 12|x_1(n)|^2|x_2(n)|^2), \tag{10}
\end{aligned}
$$
$$
\begin{aligned}
u_9^+(n) = u_3^+(n) \times {} & (4|x_1(n)|^6 + 10|x_2(n)|^6 \\
& + 30|x_1(n)|^4|x_2(n)|^2 + 40|x_1(n)|^2|x_2(n)|^4). \tag{11}
\end{aligned}
$$

Similarly, for the IM3- sub-band, the distortions terms $u_3^-(n)$ are simply obtained by interchanging $x_1(n)$ and $x_2(n)$ in (8)-(11).

The proposed DPD was based on injecting the above basis functions at the IM3+ sub-band with proper scaling such that the distortion at the IM3+ sub-band is minimized. The composite baseband equivalent PA input signal with Q^{th} order sub-band DPD processing thus reads

$$
\tilde{x}(n) = x(n) + \left[\sum_{\substack{q=3 \\ q \text{ odd}}}^{Q} \alpha_{q,n}^+ \star u_q^+(n) \right] e^{j2\pi \frac{3f_{IF}}{f_s}n} \tag{12}
$$

The qth order DPD coefficients $\alpha_{q,n}^+$ are obtained such that the correlation is minimized between the nonlinear distortion observed at the PA output at the IM3+ sub-band, and the nonlinear basis functions in (8)-(11). This is formulated as a simple block-adaptive learning approach, where the following vector based notations are defined

$$
\boldsymbol{\alpha}_q^+(m) = [\alpha_{q,0}^+(m) \ \alpha_{q,1}^+(m) \ ... \ \alpha_{q,N}^+(m)]^T, \tag{13}
$$
$$
\bar{\boldsymbol{\alpha}}^+(m) = [\boldsymbol{\alpha}_3^+(m)^T \ \boldsymbol{\alpha}_5^+(m)^T \ ... \ \boldsymbol{\alpha}_Q^+(m)^T]^T, \tag{14}
$$
$$
\mathbf{u}_q^+(n_m) = [u_q^+(n_m) \ u_q^+(n_m-1) \ ... \ u_q^+(n_m-N)]^T, \tag{15}
$$
$$
\bar{\mathbf{u}}^+(n_m) = [\mathbf{u}_3^+(n_m)^T \ \mathbf{u}_5^+(n_m)^T \ ... \ \mathbf{u}_Q^+(n_m)^T]^T, \tag{16}
$$
$$
\bar{\mathbf{U}}^+(m) = [\bar{\mathbf{u}}^+(n_m) \ ... \ \bar{\mathbf{u}}^+(n_m+M-1)], \tag{17}
$$

where N denotes the DPD filter memory depth, and n_m denotes the first sample of block m, with block size M. Consequently, the DPD block-adaptive parameter learning update then reads

$$
\mathbf{e}^+(m) = [\tilde{y}_{IM3_+}(n_m) \ ... \ \tilde{y}_{IM3_+}(n_m+M-1)]^T, \tag{18}
$$
$$
\bar{\boldsymbol{\alpha}}^+(m+1) = \bar{\boldsymbol{\alpha}}^+(m) - \mu \, \bar{\mathbf{U}}^+(m)\mathbf{e}^{+*}(m), \tag{19}
$$

where $\tilde{y}_{IM3_+}(n)$ denotes the baseband equivalent observation of the PA output at the IM3+ sub-band with the current DPD coefficients, and $\mathbf{e}^{+*}(m)$ refers to the element-wise conjugated error signal vector, while $\bar{\mathbf{U}}^+(m)$ denotes the filter input data matrix, all within the processing block m. The obtained new DPD coefficients $\bar{\boldsymbol{\alpha}}^+(m+1)$ are then applied on the next block of samples, as illustrated in [?].

In order to reduce the hardware complexity of the DPD, a sequential learning of the DPD coefficients is proposed in this paper instead of learning the DPD coefficients for all the nonlinearity orders concurrently. The idea is to first train the DPD for the third-order coefficient, and after injecting the scaled third-order basis function at the target IM3 sub-band, we start training for the fifth-order coefficient using the residual IMD at the target sub-band, and so on. This proposed learning algorithm has two advantages. The first is that only one hardware module needs to be used for training all the DPD nonlinearity orders thus reducing the hardware overhead due to DPD learning, which is an important aspect especially for small devices. The second advantage is that we can stop training the DPD once a sufficient performance is achieved. For example, if after doing the third-order training, the transmitter already satisfies the emission limits, then there is no need to train the DPD for higher orders. This will save the complexity in both the DPD training phase and in the actual DPD filtering as well.

However, for fast and smooth learning of the proposed sub-band DPD coefficients, a basis function orthogonalization procedure was proposed earlier in [?]. In this paper, we use an orthogonalization procedure which allows us to learn the DPD coefficients with different orders sequentially instead of concurrently. The idea of the orthogonalization and learning procedure in this paper is to first generate the third-order basis function and train the DPD for this basis function. Then the projection of the third-order basis function onto the fifth-order basis function is subtracted from the fifth-order basis function in order to obtain the new orthogonalized fifth-order basis function, which is then used to train the DPD for the fifth-order nonlinearity, and so on. Once the spurious emissions satisfy the emission regulations, the DPD training is stopped to save further higher-order processing that may not be required, depending on the transmission scenario and TX power level. Using the standard vector dot product, the new orthogonalized basis functions $v_q^{\pm}(n)$ used

for DPD learning thus read

$$v_3^{\pm}(n) = u_3^{\pm}(n), \tag{20}$$

$$v_5^{\pm}(n) = u_5^{\pm}(n) - \frac{dot(u_5^{\pm}(n), v_3^{\pm}(n))}{||v_3^{\pm}(n)||^2} v_3^{\pm}(n), \tag{21}$$

$$v_7^{\pm}(n) = u_7^{\pm}(n) - \frac{dot(u_7^{\pm}(n), v_3^{\pm}(n))}{||v_3^{\pm}(n)||^2} v_3^{\pm}(n) - \frac{dot(u_7^{\pm}(n), v_5^{\pm}(n))}{||v_5^{\pm}(n)||^2} v_5^{\pm}(n), \tag{22}$$

$$v_9^{\pm}(n) = u_9^{\pm}(n) - \frac{dot(u_9^{\pm}(n), v_3^{\pm}(n))}{||v_3^{\pm}(n)||^2} v_3^{\pm}(n) - \frac{dot(u_9^{\pm}(n), v_5^{\pm}(n))}{||v_5^{\pm}(n)||^2} v_5^{\pm}(n) - \frac{dot(u_9^{\pm}(n), v_7^{\pm}(n))}{||v_7^{\pm}(n)||^2} v_7^{\pm}(n). \tag{23}$$

Despite the reduced complexity that is achieved from the proposed sequential DPD learning, the learning time is now increased compared to the case when we learn all the DPD nonlinearity orders concurrently. Two algorithm modifications are thus proposed in the next section for improving the convergence speed of the proposed DPD.

4 Improving Convergence Speed of the Proposed DPD

In the previous section, a trade-off was made between hardware complexity and convergence time. We introduce two methods to help relax the extra time that is necessary to converge sequentially. Firstly, we modify the learning rate, and secondly, we modify the starting coefficients.

The first modification involves adjusting the learning rate μ in (19) depending on the residual correlation between the observed spurious IMD at the PA output and the nonlinear basis functions representing this IMD. We allow μ to take on two values, μ_1 and μ_2 where $\mu_1 > \mu_2$. This ensures fast convergence while not sacrificing the steady state error. We also establish a threshold, γ, and a confidence metric, ν. The change to μ is decided as shown in Algorithm 1. The threshold, γ, and the confidence metric ν are chosen based on experimental results over a wide range of carrier allocation scenarios and power levels. This helps ensure that the basis functions and the spurious IMD have actually decorrelated, and that we do not switch μ too soon due to fluctuations in the correlation.

The second modification involves adjusting the starting point for the DPD training. In (19), $\bar{\boldsymbol{\alpha}}(0) = \mathbf{0}$. If we were to start closer to the final coefficient, there

Algorithm 1: Adaptive μ update procedure.

$count = 0$;
$\mu = \mu_1$;
while *DPD Training* **do**
    Send block;
    Receive block;
    Calculate *correlation*;
    if *correlation* $< \gamma$ **then**
        $count = count + 1$;
    end
    if $count \geq \nu$ **then**
        $\mu = \mu_2$;
    end
end

would be less change necessary and hence the convergence time could be much faster. We propose storing the final coefficients from various transmit scenarios. Then, whenever the same or a similar transmit scenario is used again, we can retrain by starting from the previous value. The previous coefficients should be similar, but retraining allows us to overcome possible variations due to temperature, power levels, etc.

5 Overall DPD System Flow

In this section, the overall flow of the proposed DPD processing is summarized and presented, thus putting all the bits and pieces together. Fig. 2 presents a flow chart illustrating the overall DPD system processing including the iterative IM3± learning, sequential learning for the higher nonlinearity orders, as well as the convergence speed improvement proposals. In case both IM3 sub-bands are required to be suppressed, an iterative IM3± third-order sub-band DPD learning step is performed after which the spurious emissions are checked to see whether they already meet the emission requirements or not. If they do not satisfy emission requirements, an additional nonlinearity order is added with iterative IM3± learning, and so on. In all the learning phases, the DPD learning rate μ is varied according to the residual correlation between the observed IMD emissions and the corresponding basis function(s), in order to improve the learning speed, as explained in Algorithm 1. Also whenever the DPD coefficients converge, they can be stored in the memory as starting points when the transmission scenarios are repeated. In the next section, comprehensive experimental results are presented using the WarpLab setup demonstrating the effectiveness of the proposed DPD solution.
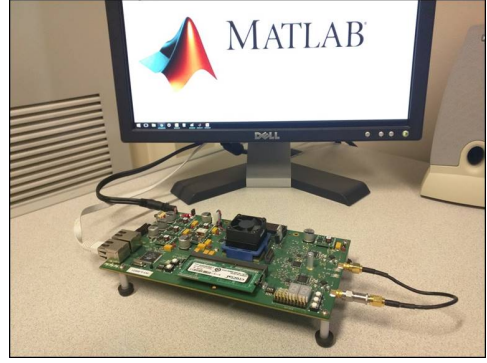

Fig. 3 The WARPv3 board interfaces with MATLAB via an Ethernet cable connected to a PC. The TX port is directly connected to the RX port with 40 dB of inline attenuation for DPD training.

6 WarpLab Results

The methods presented previously in the paper were tested using the WarpLab framework on the WARPv3 board. WARP is a software-defined radio platform that allows for rapid prototyping by interfacing with MATLAB to perform the baseband signal processing [**?**]. A photo of the experimental setup is shown in Fig. 3. For these experiments, the DPD processing is done on the host CPU, but the broadcasting is done on the WARP radio hardware which includes the Maxim MAX2829 transceiver and the Anadigics AWL6951 PA.

6.1 IM3± Iterations

We began by testing the iterative method presented in Section 2. An LTE uplink signal was generated in MATLAB with two non-contiguous carriers. One carrier was 3 MHz and the other was 1.4 MHz. Both carriers had 64 QAM subcarrier modulation. The frequency domain results at each iteration are shown in Fig. 4. The IM3+ spur was trained first using seventh-order DPD processing, and suppression was achieved as evident in the red curve. However, the IM3- spur magnitude was increased slightly which is consistent with (7). We then trained the IM3- spur (yellow curve). Again, there was a negative effect on the opposite spur, so we retrained the IM3+ spur (purple curve). At this point, we were satisfied with the performance and quit training.

6.2 Sequential Learning

As presented in Section 3, we then tested the sequential learning concept in WarpLab where we started with low-order nonlinearities and added higher orders
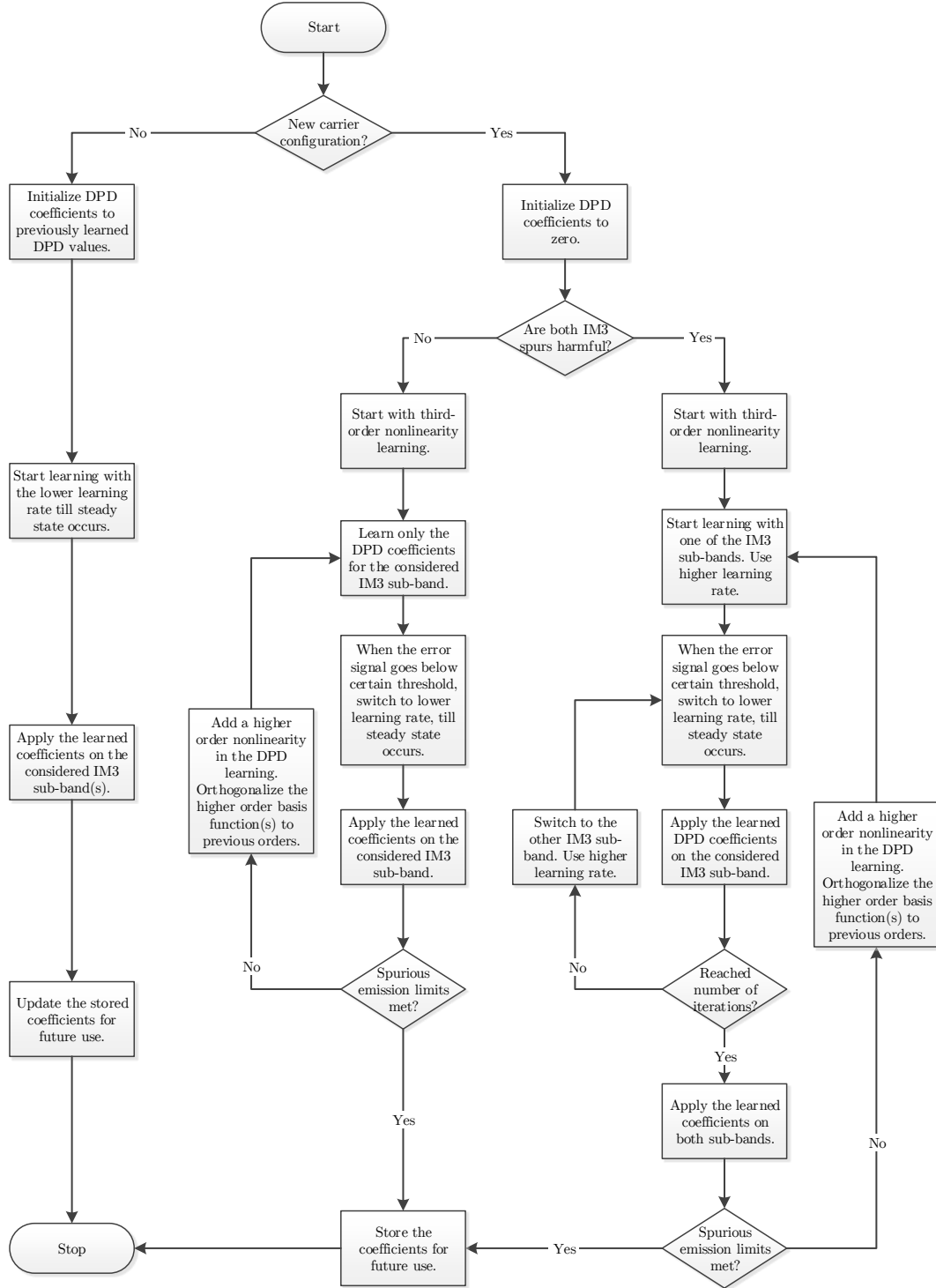
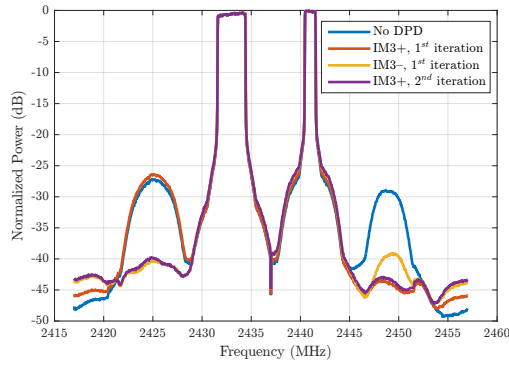**Fig. 2** Flow chart of the proposed iterative sub-band DPD solution.

Fig. 4 Normalized spectral result when using the iterative method to suppress both the IM3+ and the IM3- spurs.
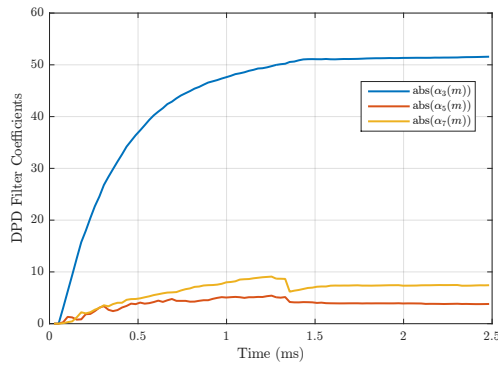

Fig. 5 Example DPD coefficient convergence when concurrent training is used. By training multiple orders concurrently, convergence occurs more rapidly at the price of additional hardware complexity when compared to sequential learning.

as needed. In Fig. 5, we show an example for comparison using the previously developed concurrent training method. We then switched to using the new sequential method as seen in Fig. 6. For these two experiments, the same LTE uplink signal and setup were used. We see that all the coefficients converged to approximately the same value. In Fig. 7, we show the results in the frequency domain on the IM3+ spur. From these figures, it is evident that the final result is equivalent and the only difference is the amount of time it takes to train.

6.3 Speed-up Methods

The convergence time for sequential training is longer than training in parallel as discussed earlier and shown in Figures 5 and 6. To overcome this, we tested the previously presented methods for speeding up the convergence time.

We tested the adaptive μ concept presented by Algorithm 1. In Fig. 8, we show the correlation between the error block and the LMS reference block as the algorithm converges. As the DPD coefficient convergences
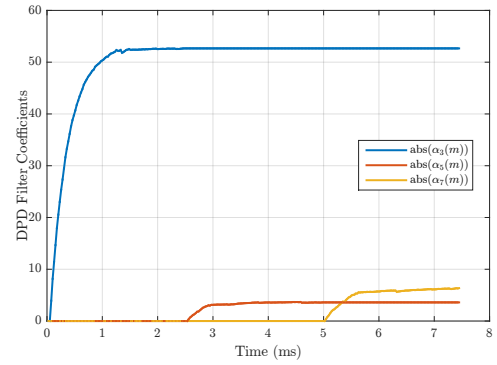

Fig. 6 WARPLab testing of sequential learning of DPD coefficients. By training multiple orders sequentially, convergence occurs more slowly with the benefit of less hardware complexity when compared to concurrent learning.
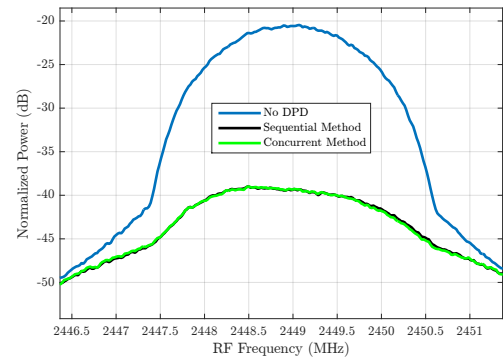

Fig. 7 PSD result when using the concurrent and sequentially trained coefficients to suppress the IM3+ spur. This shows nearly identical performance between the two methods.

(shown in blue), the correlation decreases (shown in orange). When it is below the threshold (γ) of 0.05 (shown in red) more than 5 times (the confidence metric, ν), the learning rate changes from $\mu = 4$ to $\mu = 0.7$. This change of μ is denoted by the dashed line. The values were determined experimentally to what worked well for a variety of scenarios as determined by the authors.

We then tested the concept of starting the DPD coefficient training from previous values. Using the same signal conditions as the experiment from Fig. 6, we increased the transmit power by approximately 2 dB. By doing so, we were operating in a more nonlinear region of the PA where we would have more distortion to overcome. When we broadcasted at the new power levels, the need to retrain was apparent. Without DPD, the IM3+ power was 20 dB lower than the main carriers. When using the final, converged coefficients from Fig. 6 that we obtained while training at a lower power at the new, higher transmit power, we still see suppression of the IM3+ spur. However, it was only about 11 dB of suppression. We then retrained but used the old, stale
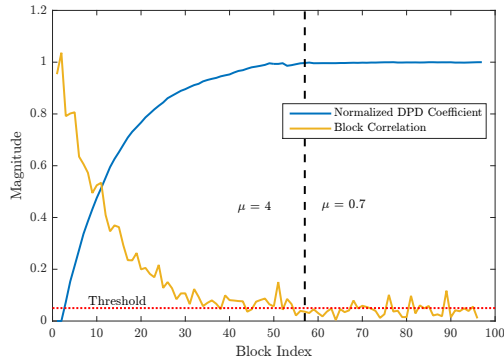
Fig. 8 Correlation vs. block index during DPD training. As training progresses the correlation decreases. Once it is below the threshold for a total number of times greater than the confidence metric, we change to the lower learning rate.
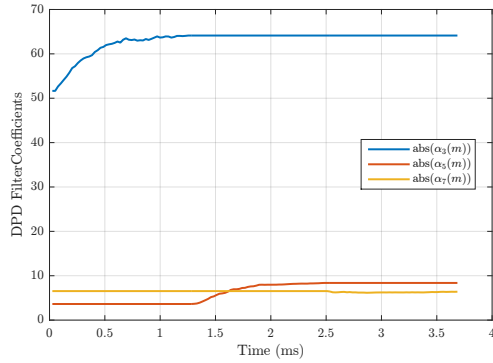

Fig. 9 Convergence of the DPD coefficients when training starts at previously obtained coefficients.

coefficients from Fig. 6 as a starting point. By doing so, we were able to reduce the amount of time necessary for convergence by a factor of 2 and obtain approximately 20 dB of suppression. The convergence of the coefficients from this experiment is shown in Fig. 9.

7 Conclusion

In this paper an iterative IM3 sub-band DPD learning algorithm has been proposed. A sequential learning procedure where higher nonlinearity orders were added one at a time was also presented in order to reduce the complexity and flexibility of the DPD. Additionally, the convergence speed of the proposed DPD has been improved by two methods, while not sacrificing the DPD performance. The first used a variable learning rate which switches from high speed to lower speed once the loop becomes close to convergence. The second method starts the DPD learning from previously learned points to reduce convergence time. A WARPLab implementation of the proposed DPD solution has been demonstrated showing excellent performance with up to 20 dB suppression in the undesired spurious emissions.